In-plane torsional stiffness in a macro-panel element for practical finite element modelling

T.Q. Li[a,*], T. Ward[a], W.J. Lewis[b]

[a] *Arup, London, UK*
[b] *University of Warwick, UK*

ARTICLE INFO

ABSTRACT

Finite element (FE) analysis produces results, which, in most cases, gain in accuracy, as the size of the FE mesh is reduced. However, this is not necessarily the case when beam and shell element connections induce in-plane torsional effects in the shell. In such situations, shell elements either do not allow for an in-plane torsional stiffness, or, when present, the in-plane torsional stiffness is incorrectly affected by the sizes of the elements. To overcome this problem, we propose a macro- panel element that has fewer degrees of freedom, includes a new model for in-plane torsional stiffness, and produces results with sufficient accuracy to meet engineering requirements. The panel element is based on the principle of sub-structuring, i.e., the panel is meshed internally by smaller shell elements. As shown in the paper, the proposed panel element can be quite large, yet, it can give accurate analysis results. This work helps to overcome a common dilemma in practical use of finite element analysis, where finite element theory requires element sizes to be sufficiently small, but practical considerations suggest the use of large-size elements that simplify the modelling process and reduce excesses in generated results. A model built using macro-panel elements is equivalent to the model built using smaller shell elements, with the normal and shear stresses in the former being the same as the stresses in the finely meshed shell element model, We identify a number of performance benefits that become available as a consequence of modelling the shell elements at a higher level of abstraction.

1. Introduction

A common conflict in practice of finite element analysis is the trade-off between the practical benefits of using larger elements against the numerical benefits of finer meshing. We have found one solution to this problem by introducing an intermediate modelling abstraction, which resulted in a 'macro-panel' element.

The proposed panel element is designed using the principle of sub-structuring: the panel is divided internally into a set of smaller shell elements. From the point of view of a user, the macro-panel element is a four node "shell" element capable of modelling large physical objects, such as a shear wall or a floor slab, with a single element. From the point of view of the finite element analysis, the panel element is a 'condensed' mesh of smaller shell elements. The macro-panel element handles the intermediate detail between the two interfaces. The proposed transformation is based upon the work in reference [1], but we have carried out further verification and validation of results to demonstrate the practical and time saving benefits.

Obtaining in-plane torsional stiffness of a shell element can become

problematic, as the stiffness is inevitably influenced by the size of the elements. We commonly observe in practice that, when a moment about the normal to a shell element is applied, the results are either not available or have poor accuracy. One typical example of this is a moment applied to shell elements via the twist of a beam perpendicularly connected to them. The larger size of the proposed macro-panel element makes it possible to conveniently accommodate the in-plane torsional moments over a wider area and predict the in-plane torsional stiffness more accurately. In this paper, we recommend a new method for calculating the in-plane torsional stiffness that makes use of the larger area offered by the transformation into a macro-panel element. We have found that this method produces greater accuracy than previously proposed methods (refs. [2–7]), in which the in-plane torsional stiffness is more sensitive to individual element sizes. To account for the situation where an in-plane torsional stiffness is not required, we make the inclusion of in-plane torsional stiffness optional by means of a user-defined parameter.

We demonstrate the effectiveness and applicability of the proposed macro-panel element model using two key examples. In Example 1, we

model a 40-storey structure with linked shear walls and compare the results with three alternative finite element models that use shell elements to represent the walls and beam elements to represent the links. The alternative models given in this example include Allman/Cook formulation with in-plane torsional stiffness, as well as shell elements without that stiffness. In Example 2, we model a shear wall core of a 30-storey building subjected to horizontal uniform face loads. The core is modelled using the proposed macro-panel element model and the results are compared with the shell element model.

The results show that our proposed macro-panel element offers a number of benefits. Other than facilitating a more accurate method for predicting the in-plane torsional stiffness, while retaining the quality of a finely meshed model, it offers real practical advantages. The data associated with each panel element is independent and so the processing of any panel can be executed independently in a parallel way. We also find a reduction in the repetitive calculations of any individual panel, since it is only necessary to process a single element. Finally, we commonly observe a reduction possible at the structural level where we have found it very likely that in a large structural model, many identical panels exist, but where only one of them needs to be processed.

2. The macro-panel element

2.1. Meshing of the panel element

The macro-panel element represents a substructure with internal meshing of shell elements at an arbitrary degree of refinement. Example refinements may represent a single panel by 4×4, 4×6 or 6×6 etc. shell elements. We restrict the discussion in this paper to a meshing scheme of 4×4 Quad8 shell elements, whose 'internal' assembly is shown in Fig. 1(a). The rectangular shape of the panel element is used here, but the method does not limit the shape to be rectangular and any quadrilateral shape can be used. We refer to all nodes within the panel element as 'internal' nodes, and reserve the name 'external' for all remaining nodes that are at the panel edges and corners. The node numbering is from internal nodes to edge nodes, and then the four corner nodes. Fig. 1(b) shows the 'external' nodes of the panel element as given to the global assembly where only these nodes will be active (the nodes have been re-numbered, for convenience). Fig. 1(c) shows the macro-panel element as seen by the end user; it is a typical four-node 2D element, and the four nodes are also re-numbered from one. The numbers shown in brackets indicate the degrees of freedom number.

All degrees of freedom (d.o.f.) associated with internal nodes are 'condensed' during the macro-panel element construction and do not appear in the global analysis. As a consequence, the total number of d.o.f. is significantly reduced (compared to the equivalent model that is using smaller shell elements).

The derivation of an individual shell element stiffness matrix $[K_e]$ can be found from a variety of sources e.g. reference [8] and is not discussed here. In this paper we concentrate on the idea of the panel element as a larger entity: the assembly of the macro-panel element stiffness matrix, the assembly of a corresponding load vector, and a method of constructing the in-plane torsional stiffness from the internal arrangement.

2.2. Stiffness matrix of the macro-panel element

Given a known stiffness matrix $[K_e]$ of a shell element (refer to Section 13.2 on pages 428 & 429 of reference [8]) for detailed derivation) and the element numbering system shown in Fig. 1(a), the stiffness matrix of the meshed panel in Fig. 1(a) can be assembled and partitioned by internal and external d.o.f. and take the following form:

$$[K] = \begin{bmatrix} K_{ii} & K_{ib} \\ K_{bi} & K_{bb} \end{bmatrix} \tag{1}$$

For the meshing scheme shown in Fig. 1(a), i is from 1 to 165 for the 33 internal nodes and each has 5 d.o.f., b is from 166 to 357 for the 32 external nodes and each has 6 d.o.f.

Using Guyan condensation method [9] to eliminate the internal d.o.f., the final stiffness matrix of the panel element with only external nodes can be obtained from:

$$[K^e] = [K]_{bb} - [K]_{bi}[K]_{ii}^{-1}[K]_{ib} \tag{2}$$

where the total number of d.o.f. of the panel element is 192- corresponding to the 32 external nodes (the node and d.o.f. numbering system for the panel element is shown in Fig. 1(b); Fig. 1(c) shows the node and d.o.f. numbering for the panel element as seen by the end user).

We can see from this example that the number of d.o.f. of the panel element is 192, while the total number of d.o.f. of the meshed model is 390. This shows that the total number of d.o.f. has been reduced by a half in this example. Consequently, for a structure modelled using panel elements, the size of the global stiffness matrix can be significantly reduced, producing time saving benefit in solving the matrix equation problem. The code routines for assembling the stiffness matrix of the meshed panel and then condensing the stiffness matrix to panel element stiffness matrix with only external d.o.f. active is based on reference [1] and can be found in the Appendix.

2.3. Load vector of the panel element

If there are distributed loads on the panel elements, the loads have to be represented by nodal loads in the analysis. The nodal loads act on both internal and external nodes. As internal nodes are not active in global analysis, the nodal loads also need to be condensed to external nodes in the similar way as condensing the stiffness matrix. Given a known nodal load vector $\{P\}$ for the meshed model, we can partition the load vector into an internal block $\{P\}_i$ followed by an external block $\{P\}_b$. The condensed nodal load vector $\{P\}_b'$ at only external nodes for global analysis can be obtained from:

$$\{P\}_b' = \{P\}_b - [K]_{bi}[K]_{ii}^{-1}\{P\}_i \tag{3}$$

where:

$\{P\}_b$ The external block of the nodal load vector, the length is 192 for the example.
$\{P\}_i$ The internal block of the nodal load vector, the length is 165 for the example.
$\{P\}_b'$ The condensed load vector at external nodes for global analysis. The length is 192 for the example discussed.
$[K]_{bi}$ Defined by Eq. (1)
$[K]_{ii}$ Defined by Eq. (1)

In practice $\{P\}_b'$ is not derived directly from Eq. (3), but gained in the same process of condensing stiffness matrix $[K]$, and the code routines can also be found from reference [1] and Appendix. When multiple load cases exist, the load vectors become a load matrix and each load vector is represented by a single column in the load matrix.
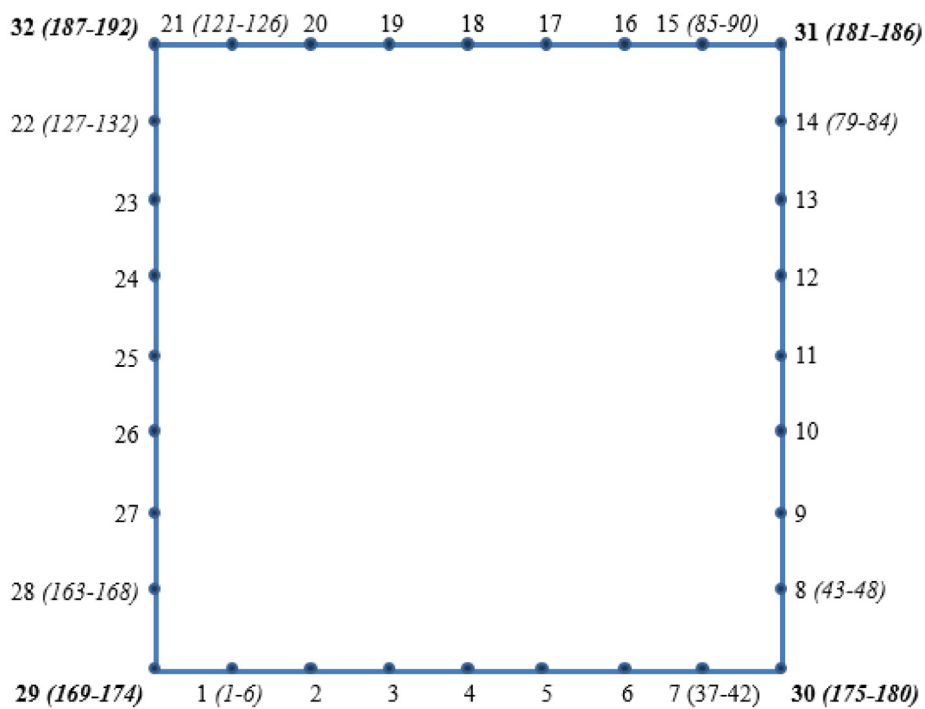
3. Analysis results of the panel element

3.1. Nodal displacements

Given the condensed stiffness matrix $[K]_{bb}'$ and condensed load vector $\{P\}_b'$, a global stiffness matrix and global load vectors for the whole structural model can be assembled and the matrix equilibrium equation can be solved in the usual way [8]. The displacements from
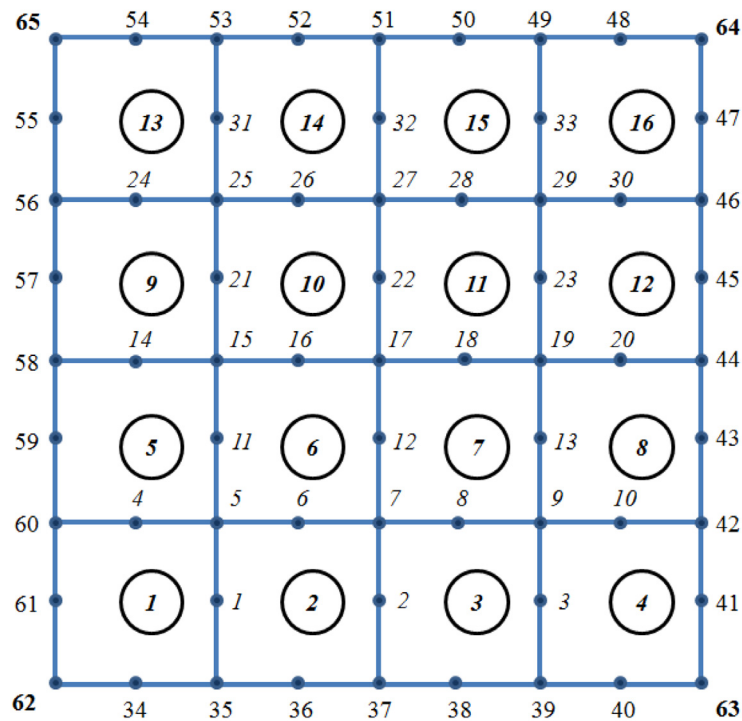
(a) Meshing of the macro-panel element: node and element numbering

(b) Macro-panel element used by the solver in global analysis.

(Numbers in brackets indicate nodal d.o.f.)

Fig. 1. Macro-panel element and the meshing scheme.

global analysis are the node displacements $\{u\}_b$ of the external nodes of the panel elements. The internal node displacements $\{u\}_i$ of the panel elements are not required if stress and force results within the panel elements are of no interest, e.g. when only the total edge forces and moments given below are needed to calculate the reinforcement. If

stresses and forces within the panel elements are required, internal node displacements need to be known and they can be determined from:

$$\{u\}_i' = [K]_{ii}^{-1}[P]_i + [K]_{ii}^{-1}[K]_{ib}\{u\}_b \tag{4}$$
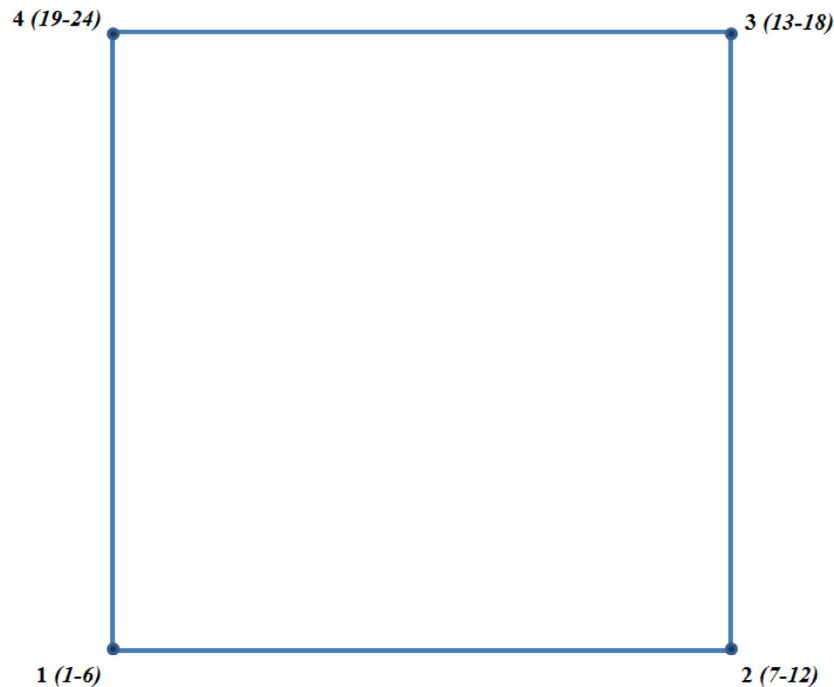
(c) Macro-panel element available to a user

Fig. 1. (*continued*)

where:

 $\{u\}'_i$ The nodal displacement vector of internal nodes.
 $\{u\}_b$ The nodal displacement vector of external nodes.

All other parameters are the same as in the equations above.

The first term on the right hand side of Eq. (4) represents the contribution to internal node displacement vector due to the loading of internal nodes, in the absence of any external node displacement. The second term represents the contribution to internal node displacement vector due to the displacements at external nodes, in the absence of any other loads.

3.2. Total forces/moments at edges

Once nodal displacements of external nodes are known, forces and moments at those nodes can be calculated from

$$\{F\}_b = [K]'_{bb}\{u\}_b \tag{5}$$

where:

 $\{F\}_b$ The force vector representing the forces/moments at external node.
 $\{u\}_b$ The external node displacement vector.

$\{F\}_b$ can then be used to calculate the total forces and moments about the centroid of the four edges of the panel element.

In engineering design, it may happen that the resultant value of forces and moments about the centroid of a section is more useful than a detailed stress distribution across the section. One example may be the calculation of required reinforcements for a shear wall subjected to mainly in-plane forces. In such situations, a macro-panel element is a natural fit; should a single panel element represent a wall or slab, the total forces and moments at a panel edge immediately represent the total forces and moments for a section through the structural object.

Edge forces and moments can be calculated from the known forces and moments at external nodes given by Eq. (5). Fig. 2 shows an option for a sign convention for representing total panel element edge forces and moments.

3.3. Forces, moments, stresses & strains within the element

When the panel element is used to model a shear wall, the total forces and moments at the edges are typically sufficient for the purpose of engineering design. When a panel element is used to model floors and other structural objects subjected to out-of-plane bending, greater detail as to the forces, moments, stresses and strains within a panel element will typically be required. Given that the panel element is represented internally by shell element mesh, the strains and stresses within the panel can be calculated from each of shell elements in the meshed model shown in Fig. 1(a).

4. In-plane torsional stiffness

4.1. Introduction

A node of a typical shell element has five degrees of freedom, three translations and two rotations. Resistance to rotations about the normal to the element plane, commonly referred to as in-plane torsional stiffness is not usually included. If such shell elements are used in an otherwise unrestrained global assembly with six degrees of freedom (three translations and three rotations) of each node, some additional method of constraint will be necessary. At the global analysis stage, if connected shell elements are exactly co-planar, it is straightforward to automatically suppress the unwanted in-plane torsional d.o.f. and have only 5 d.o.f. for each node in the analysis. Alternatively, a small artificial in-plane torsional stiffness may be assumed, so as to keep all six d.o.f. for each node in the global assembly. Should two connecting shell elements be perpendicular, the connecting nodes, each with six degrees
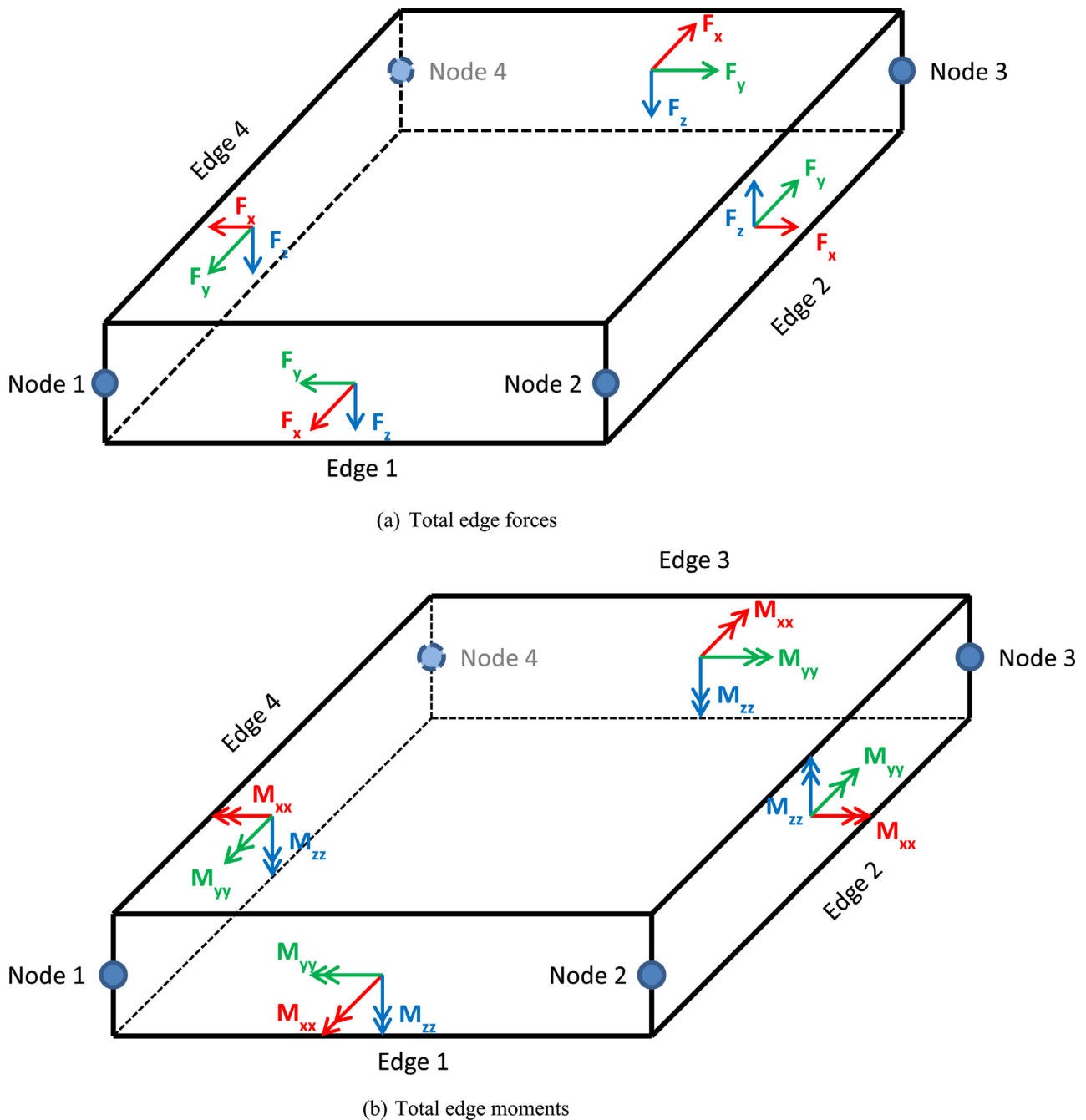
(a) Total edge forces

(b) Total edge moments

Fig. 2. Sign convention for representing total forces and moments at the panel element edges.

of freedom, will have an associated stiffness. A greater problem occurs when all shell elements connected to a node are not co-planar, but nearly co-planar. In this case, the small rotational stiffness about the normal direction contributed by the connected elements is likely to lead to poor conditioning in the resulting global stiffness matrix for the structure. The alternative approach of suppressing the non-zero rotational stiffness about the normal direction will, likewise, lead to unsatisfactory results.

Solutions introduced by Allman and Cook include the in-plane torsional d.o.f. as a part of the element formulation [2–7]. The technique is to include four mid-side nodes with transverse mid-side displacements that are instead expressed as four rotational d.o.f. at element corner nodes. The method is effective, but under certain conditions: when

elements are reasonably co-planar [10], spurious modes are handled effectively [7], and the element size is sufficiently large with respect to the area over which the in-plane torsional moment is applied.

In practice, however, we observe conflict between the requirement to refine element mesh sufficiently and at the same time keep element sizes large enough to accommodate the possibility of applying in-plane torsional moments over single connections. We have found that overly small elements can be a poor compromise in practical situations. For an Allman/Cook element [7], Fig. 3 demonstrates the effect of element size on the rotation at a node when a constant in-plane torsional moment is applied. We can see the rotation at centre node varies significantly with the variation of shell element size. This implies that, in order to have correct in-plane torsional stiffness, a certain shell element size has to be
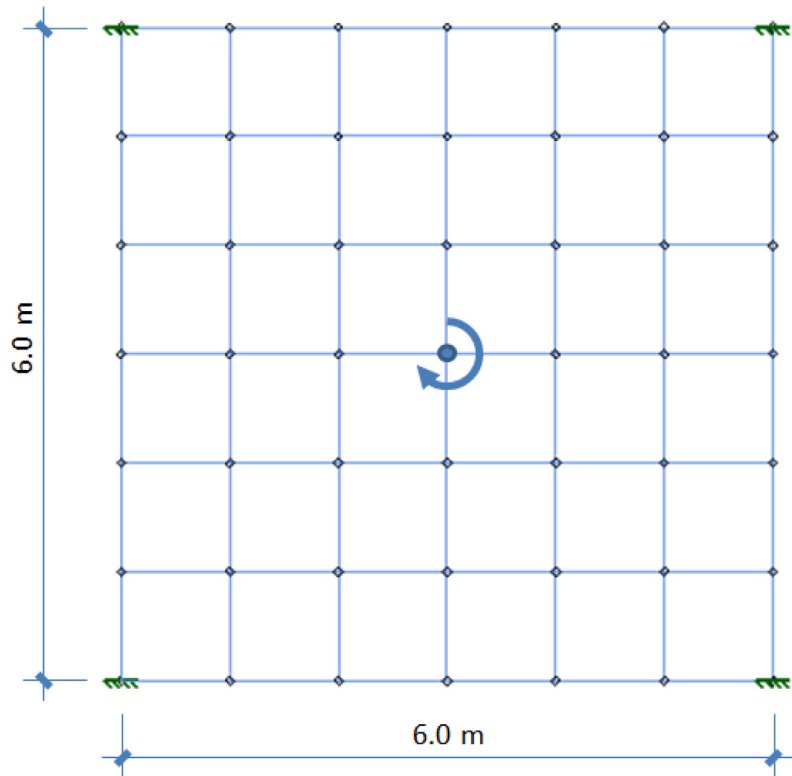
(a) The model (thickness = 0.5 m, $E = 2.8 \times 10^{10}$ Pa, Moment = 1×10^{6} N.m)
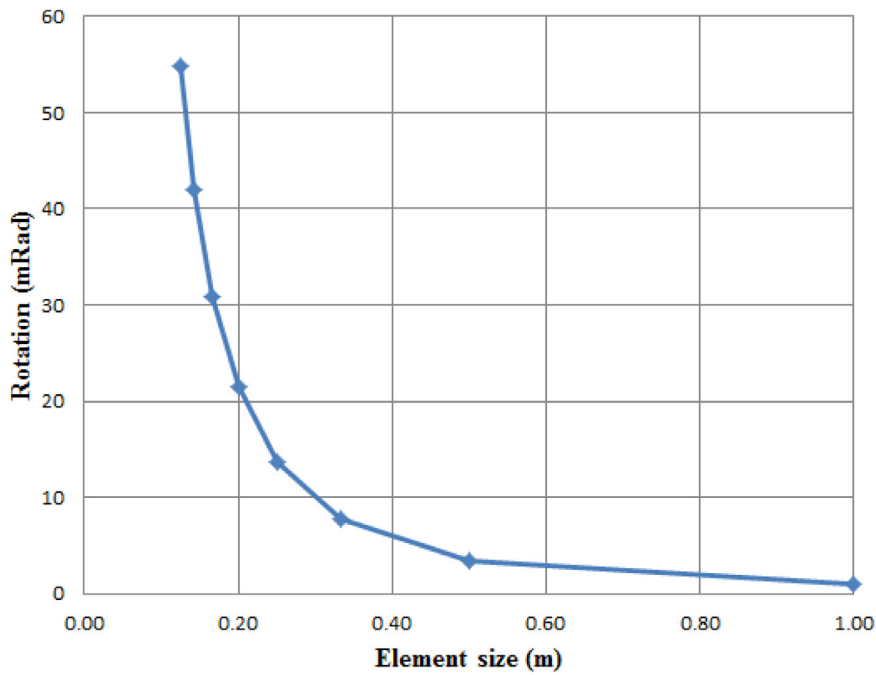

(b) Rotation versus element size for a constant value of applied moment

Fig. 3. Effect of element size on in-plane torsional stiffness using Allman/Cook method.

used and this is not practically possible within rather fine meshing. The macro-panel element, working at a higher level of model abstraction, has a greater opportunity to consider the section size of a connecting beam in the process of deriving the in-plane torsional stiffness of the panel. In this paper a beam section size is taken as an additional parameter of the panel element to enable the correct in-plane torsional stiffness to be derived.
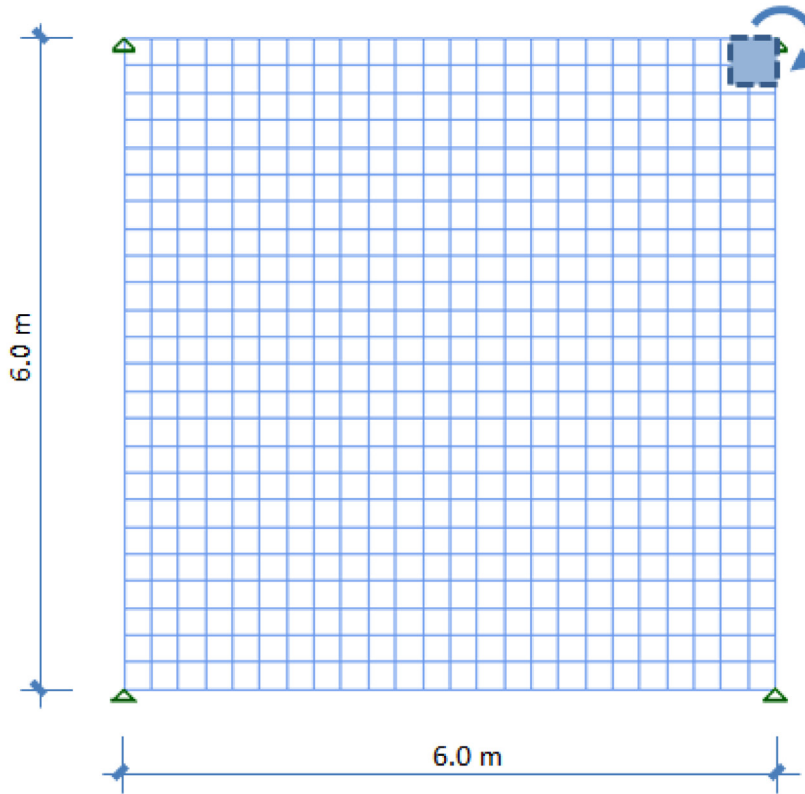
(a) The model (thickness = 0.5 m, E = 2.8×10^{10} Pa)
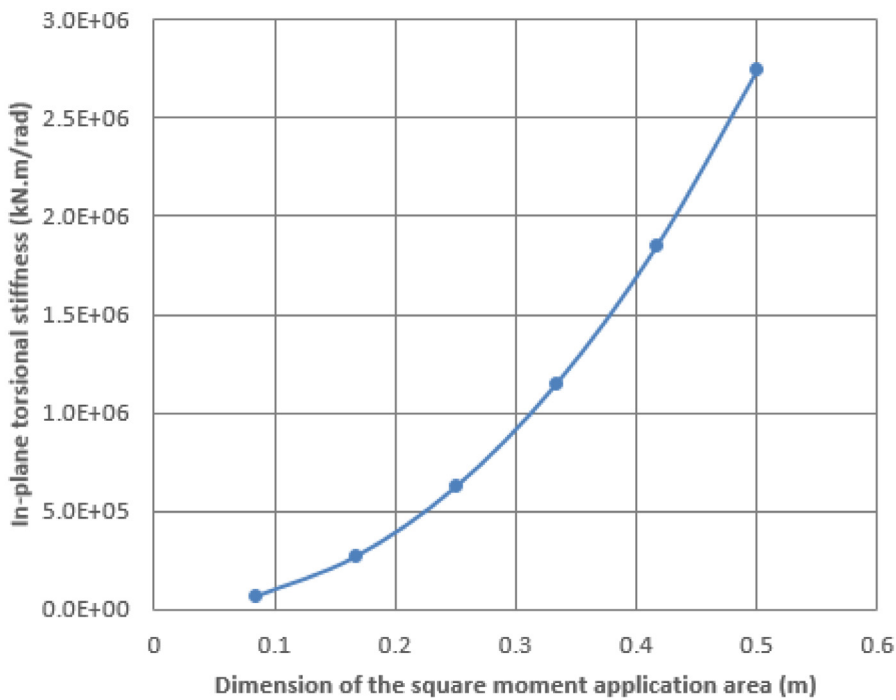
(b) In-plane torsional stiffness versus moment application area

Fig. 4. Effect of moment application area on the in-plane torsional stiffness.

4.2. Derivation of in-plane torsional stiffness

Fig. 4 demonstrates the effect that an area over which an in-plane torsional moment is applied has on the in-plane torsional stiffness of the panel. In this example, a square 6 × 6 m panel is modelled by a finer mesh of Quad8 shell elements. A set of in-plane torsional moments is applied to the top right corner with varying application areas. The relationship between the in-plane torsional stiffness and the application
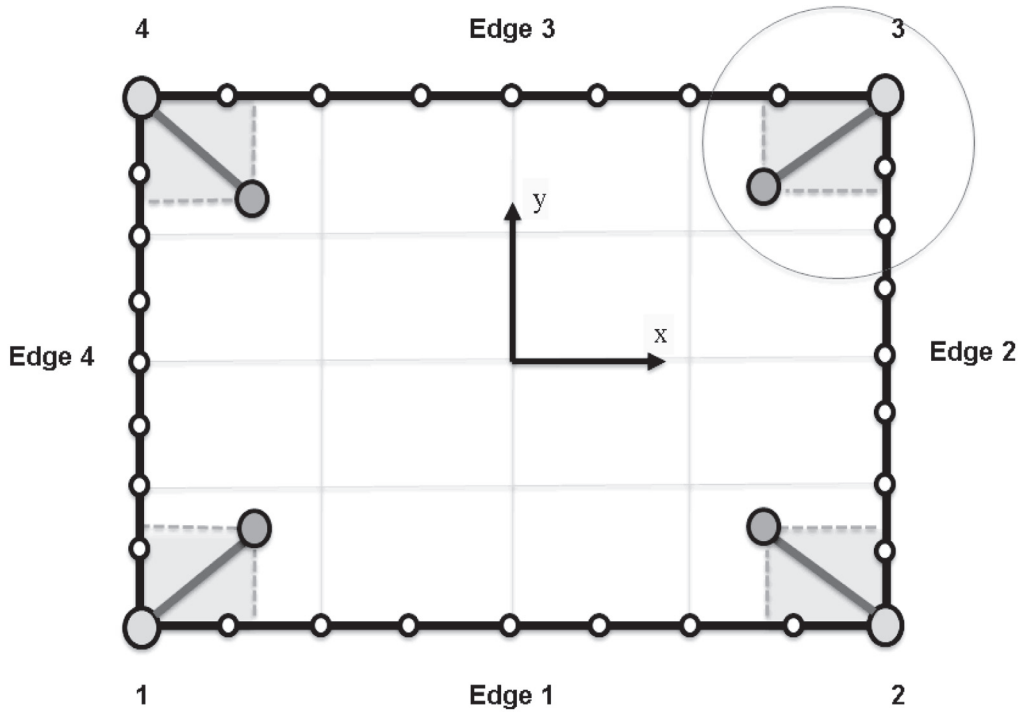
(a) The model of the macro-panel element with dummy nodes and rigid bars
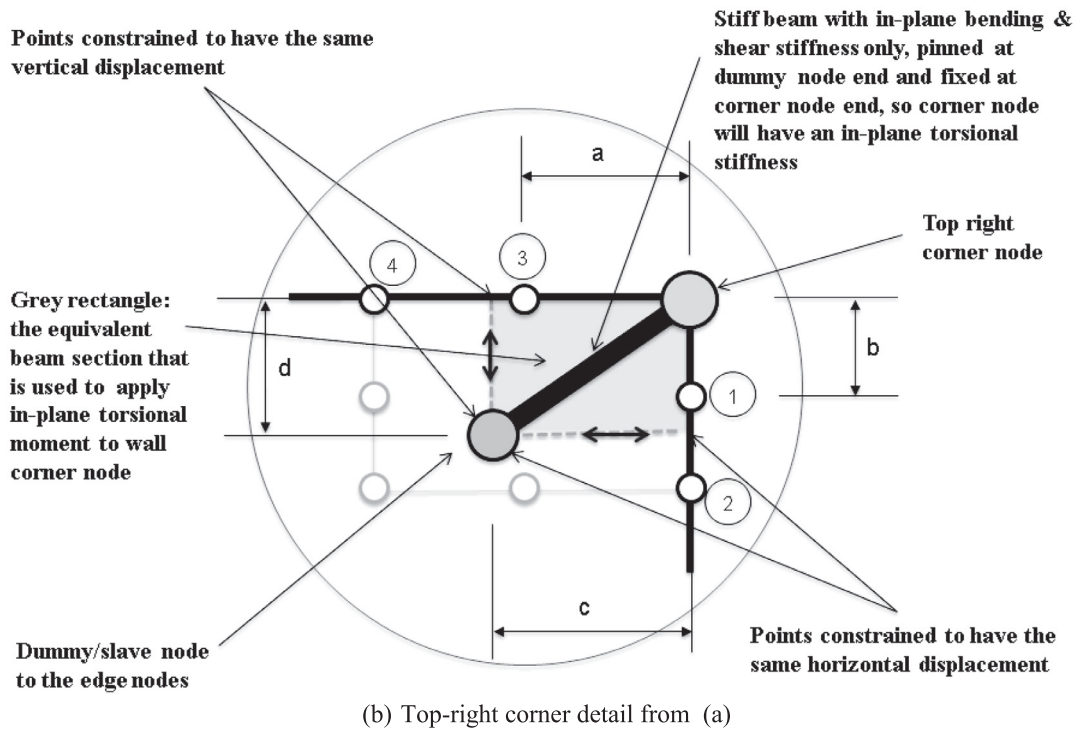
(b) Top-right corner detail from (a)

Fig. 5. The internal arrangement to facilitate the generation of in-plane torsional stiffness.

area of the in-plane torsional moment is drawn in Fig. 4(b). It shows that the moment application area does have significant effect on the in-plane torsional stiffness. This means that, in practice, the moment application area has to be considered in order to obtain the correct in-plane torsional stiffness.

The derivation of the in-plane torsional stiffness for a panel element is illustrated in Fig. 5. A 'dummy' node lying within the panel element plane and containing the two in-plane translational d.o.f. is placed near
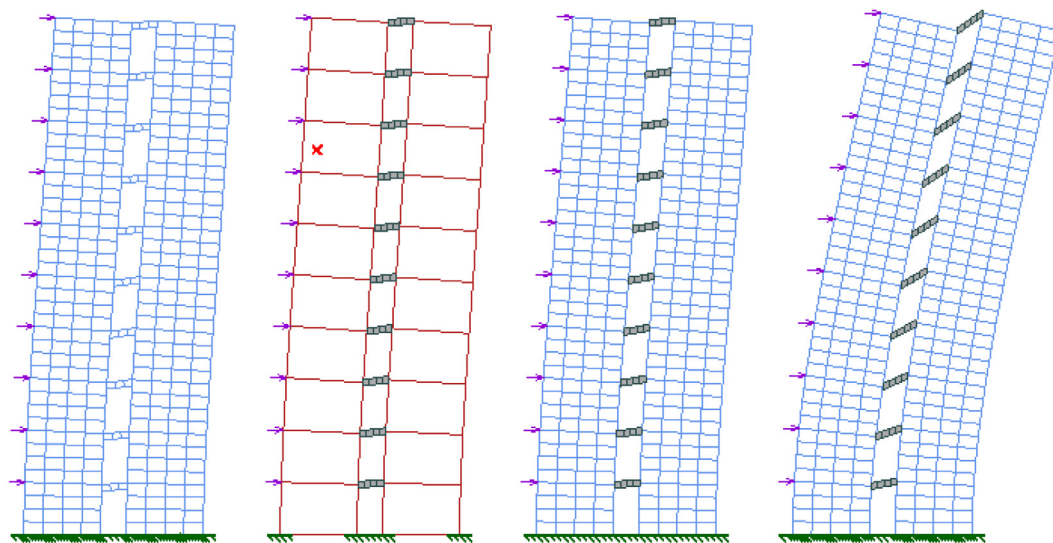
Model I   Model II   Model III   Model IV

total height   = 40 m;   total width = 14 m;   link length   = 2 m
wall thickness   = 200 mm;   material E = 2.8x10^{10} N/m^2 one point load   = 30 kN

Fig. 6. The linked shear wall models with deformed shapes.

each corner. In this way, an area over which an in-plane torsional moment is to be applied can be flexibly specified by defining the distance between the dummy node and the element edges; for example: c & d in Fig. 5(b). This area may be set as the equivalent section area of a connecting beam element. The displacement of each dummy node is constrained to be equal to the corresponding edge point displacements as shown in Fig. 5(b). If the edge point does not coincide with an edge node, linear interpolation can be used to get the edge point displacements. For example, the displacements of the dummy node at the top right corner in Fig. 5 are constrained according to the following equations:

$$u_x = u_{1.x} + \frac{(u_{2.x} - u_{1.x})}{b}(d - b)$$

$$u_y = u_{3.x} + \frac{(u_{4.x} - u_{3.x})}{a}(c - a) \tag{6}$$

where:

u$_x$, u$_y$ Horizontal and vertical displacements of the dummy node.
u$_{1.x}$, u$_{2.x}$ Horizontal displacements at edge nodes 1 & 2, as shown in Fig. 5(b).
u$_{3.y}$, u$_{4.y}$ Vertical displacements at edge nodes 3 & 4 as shown in Fig. 5(b).
a, b The nodal spacing at horizontal and vertical edges respectively.
c, d The width and height of the rectangular moment application area.

Each dummy node is linked to its respective corner node by a stiff beam element in order that each corner node has an in-plane torsional stiffness allowing it to resist the moment applied through the area determined by c and d. The stiff beam element has a large in-plane bending and shear stiffness, but no axial or out-of-plane bending stiffness. We have found this simpler approach to be sufficient in practice to produce in-plane torsional stiffness for the corner nodes. Dummy node displacements are restrained and they do not have independent d.o.f.,

so their introduction does not change the total number of d.o.f. in the panel element.

5. Worked examples

The proposed macro-panel element has been implemented in the structural finite element software *Oasys GSA* [11]. In this section, we present two worked examples. Example 1 is a linked shear wall modelled by the proposed panel elements as well as by usual, smaller size, shell and beam elements. Example 2 is a 30- storey shear wall core modelled by the proposed panel elements and smaller size shell elements.

Example 1
Four finite element models of the same linked shear wall are created in Oasys GSA and they are:

(I) Full shell element model – shell elements are used to model both the shear walls and the links, this model is used as the benchmark to calibrate other model's analysis results
(II) Panel element model – panel elements are used to model the shear walls and beam elements are used to model the links
(III) Allman/Cook model – shell elements are used to model the shear walls, and beam elements are used to model the links. Allman/Cook formulation is used for shell elements to include in-plane torsional stiffness
(IV) Non-Allman/Cook model – the same as Allman/Cook model except that bilinear formulation is used for shell elements and the shell elements have no in-plane torsional stiffness

The geometries, loading and the deformed shapes of the four models are shown in Fig. 6. The displacements at each floor level from the four models are summarised in Table 1. They show that the panel element model (model II) gives very similar displacements to the full shell element model (model I). This demonstrates that the panel elements can

uniform face load = 1.0 kN/m²

6 m

4 m   4 m   4 m
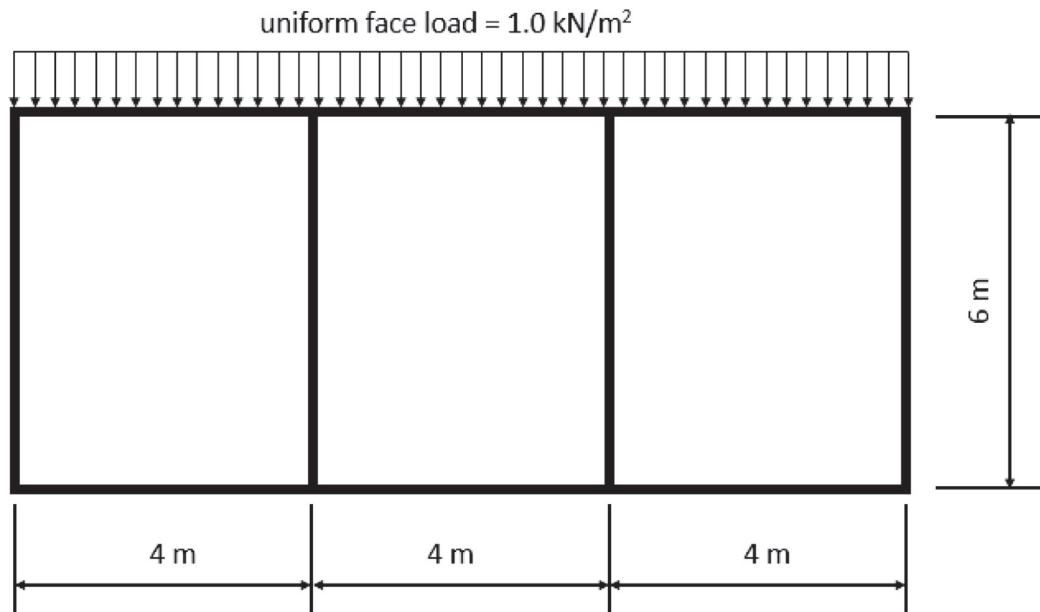
number of stories = 30	storey height = 3 m;
wall thickness = 0.25 m	material E = 1.4x10¹⁰ N/m²

Fig. 7. The plan view of the shear wall core.

Table 1
Horizontal displacements predicted by the four models.

Floor Level	Full shell element model (Model I) (mm)	Panel element model (Model II) (mm)	% diff	Allman/Cook model (Model III) (mm)	% diff	Non-Allman/Cook model (Model IV) (mm)	% diff
1	0.20	0.19	−1.78%	0.21	5.63%	0.33	65.23%
2	0.55	0.55	−0.31%	0.60	9.32%	1.05	90.35%
3	1.02	1.02	0.10%	1.13	11.19%	2.10	106.48%
4	1.56	1.56	0.32%	1.75	12.52%	3.43	119.83%
5	2.13	2.14	0.38%	2.42	13.51%	4.94	131.80%
6	2.71	2.73	0.44%	3.10	14.37%	6.60	143.18%
7	3.29	3.30	0.49%	3.79	15.18%	8.35	153.95%
8	3.84	3.86	0.52%	4.45	15.90%	10.16	164.38%
9	4.38	4.40	0.53%	5.10	16.61%	11.99	173.93%
10	4.92	4.95	0.57%	5.77	17.17%	13.85	181.45%

Note: see Fig. 6 for the dimensions and material properties of the models.

accurately model the linked shear wall and also predict the in-plane torsional stiffness accurately. Only 20 panel elements and 10 beam elements are used in the panel element model, which makes the modelling much simpler than using shell elements where 350 shell elements are needed; this shows the efficiency of using panel elements in modelling this linked shear wall and similar types of structures.

The non-Allman/Cook model (model IV) gives excessively large displacement; this is obviously due to the fact that the shell elements have no in-plane torsional stiffness. Because of this, the two branches of the shear walls are working alone without effectively linked as an integral wall. The Allman/Cook model (model III) does exhibit some degree of in-plane torsional stiffness, but the in-plane torsional stiffness is under estimated as the displacements are much larger than full shell element model. If the shell element sizes become smaller, the error of in-plane torsional stiffness will be even larger, as the in-plane torsional stiffness from Allman/Cook method reduces along with the reduction of

element size. This shows the limitation of using Allman/Cook method to predict the in-plane torsional stiffness in practical uses.

Example 2

A shear wall core subjected to horizontal uniform face loads is shown in the Fig. 7. The plan view, the dimensions and material properties of the shear wall core are shown in the same figure. The storey height is 3 m and the total number of stories is 30. The core is modelled using the proposed panel element model as well as small shell elements. In the panel element model, each wall measured from one floor to the next is modelled by a single panel element; in the shell element model, the same wall is modelled by 4 by 4 small shell elements, equal to the meshed elements within the panel element.

The horizontal displacements of the two models (at the floor level) are summarised in Table 2. They show that the panel element model gives almost the same displacements as the shell element model, even though the number of elements used in the panel element model is only

Table 2
Horizontal displacements predicted by the shell element and panel element models.

Floor Level	Shell element model (mm)	Panel element model (mm)	difference (%)
1	0.330	0.333	0.88%
2	1.029	1.034	0.49%
3	2.096	2.103	0.33%
4	3.509	3.517	0.23%
5	5.243	5.253	0.19%
6	7.277	7.288	0.15%
7	9.586	9.599	0.14%
8	12.150	12.160	0.08%
9	14.940	14.960	0.13%
10	17.950	17.960	0.06%
11	21.140	21.160	0.09%
12	24.510	24.530	0.08%
13	28.030	28.050	0.07%
14	31.690	31.700	0.03%
15	35.470	35.480	0.03%
16	39.350	39.370	0.05%
17	43.330	43.350	0.05%
18	47.380	47.400	0.04%
19	51.500	51.520	0.04%
20	55.680	55.700	0.04%
21	59.900	59.930	0.05%
22	64.160	64.180	0.03%
23	68.450	68.470	0.03%
24	72.760	72.780	0.03%
25	77.080	77.100	0.03%
26	81.410	81.440	0.04%
27	85.750	85.770	0.02%
28	90.090	90.110	0.02%
29	94.420	94.450	0.03%
30	98.760	98.790	0.03%

Note: see Fig. 7 for the dimensions and material properties of the models.

1/16 of the shell element model. This demonstrates the efficiency of using the proposed panel elements to model this type of structure.

The average times used to solve the four models in Example 1 and the two models in Example 2 using Dell Latitude E7250 lap top are given in Tables 3 and 4 respectively. They show that analysing the panel element model needs shorter time compared with shell element models. This is due to the fact that panel element model has a smaller number of global d.o.f. and also has fewer repetitive calculations, as all

Table 3
Solver time of the 4 models in Example 1.

	Full shell element model Model I	Panel element model Model II	Allman/Cook model Model III	Non-Allman/ Cook model Model IV
Analysis time (s)	0.71	0.39	0.49	0.47

Table 4
Solver time of the 2 models in Example 2.

	Shell element model	Panel element model
Analysis time (s)	6.16	3.52

panel elements are the same and only one panel element needs to be processed.

6. Conclusions

To an engineer, being able to work at a higher level of abstraction, offered by the proposed macro-panel element presents the immediate benefit of the model being easier to construct, manipulate and maintain. The proposed method can predict in-plane torsional stiffness accurately by taking advantage of large size of the panel elements. Panel element results can be presented at a level that matches physicality of structural objects, such as walls & slabs, with total forces and moments at the panel edges that may reflect a cut section of a wall. The size of the digital model and the volume of s results that require analysis are also significantly reduced.

For the finite element solver, the use of larger and repeated structural objects (the panel elements) provides a natural opportunity for performance improvements, especially when using multiple cores of modern computers. The proposed model handles the calculations within the panel elements and passes a reduced number of d.o.f. to the global assembly; this reduces the total number of d.o.f. in global analysis and saves time in solving the global stiffness matrix. In our simple example, the overall time reduction of solving the problem using panel elements is about 40%. For larger, regular models, and using multiple processors, the saving of analysis time would be much higher.

Appendix

From the known stiffness matrix K_e of shell elements and the numbering system of nodes and elements shown in Fig. 1(a), the stiffness matrix K of the meshed model of Fig. 1(a) can be assembled using the routine shown below in C++. Five d.o.f. are used at each node, except for the corner nodes that have six d.o.f.

```
void AssembleK(std::vector<std::vector<double>>& K)
{
  for(int iE = 0; iE < 16; ++iE)
  {
    for(int iR = 0; iR < 40; ++iR)
    {
      for(int iC = 0; iC < 40; ++iC)
      {
        const int iTR = vTopo[iE][iR/5];
        const int iTC = vTopo[iE][iC/5];
        int iRG = 5*(iTR-1) + iR%5;
        int iCG = 5*(iTC-1) + iC%5;
```

```
                  if(iTR > = 62)
                    iRG = 6*(iTR-1) + iR%5 - 61;
                  if(iTC > = 62)
                    iCG = 6*(iTC-1) + iC%5 - 61;
                    K[iRG][iCG] + = Ke[iR][iC];
              }
          }
      }
  }
```

where:

vTopo: A vector holding the topologies (node numbers) of each of the small shell elements as shown in Fig. 1(a), e.g. vTopo [1,2], gives the second node number of element 1.
K_e: The small shell element stiffness matrix of size 40×40.
K: The stiffness matrix of the meshed model (uncondensed)

Using the numbering system shown in Fig. 1(a), the internal and external degrees of freedom are separated automatically in the meshed model stiffness matrix K, with internal d.o.f. followed by external d.o.f. The total number of d.o.f. for the meshed model is $N_t = 329$ and the number of internal d.o.f. $N_i = 165$. The uncondensed stiffness matrix K and the corresponding load vectors can be condensed using the following routine.

```
void CondenseMatrix(std::vector < std::vector < double > >& K, std::vector < std::vector < double > >& P, int Nt, int Np, int Ni)
{
      for(int k = 0; k < Ni; + +k)
    {
      for(int i = k + 1; i < Nt; + +i)
      {
        const double dFactor = K[i][k]/K[k][k];
        for(int j = k; j < Nt; + +j)
          K[i][j] = K[i][j] - dFactor*K[k][j];
        for(int j = 0; j < Np; + +j)
          P[i][j] = P[i][j] - dFactor*P[k][j];
      }
    }
      for(int k = Ni-1; k > 0; --k)
    {
        for(int i = k-1; i > = 0; --i)
      {
        double dFactor = K[i][k]/K[k][k];
        for(int j = 0; j < Nt; + +j)
          K[i][j] = K[i][j] - dFactor*K[k][j];
        for(int j = 0; j < Np; j++)
          P[i][j] = P[i][j] - dFactor*P[k][j];
      }
    }
      for(int i = 0; i < Ni; + +i)
    {
        const double dFactor = K[i][i];
        for(int j = 0; j < Nt; j++)
          K[i][j] = K[i][j]/dFactor;
        for(int j = 0; j < Np; j++)
          P[i][j] = P[i][j]/dFactor;
    }
  }
```

where:

Nt: The number of d.o.f. in the meshed model (329 in this example).

Ni: The number of internal d.o.f. (165 in this example).

Np: The number of load cases considered.

K: The stiffness matrix. At the start, K contains the stiffness matrix of the meshed model, assembled using the routine above. At the end, K contains:

$$[K] = \begin{bmatrix} [1] & [K]'_{ib} \\ [0] & [K]'_{bb} \end{bmatrix} = \begin{bmatrix} [1] & [K]_{ii}^{-1}[K]_{ib} \\ [0] & [K]_{bb} - [K]_{bi}[K]_{ii}^{-1}[K]_{ib} \end{bmatrix}$$

(A1)

P The load matrix. Each column represents a load case. At start, P holds the load matrix for the meshed model, at the end P contains:

$$[P] = \begin{bmatrix} [u]^i_i \\ [P]'_b \end{bmatrix} = \begin{bmatrix} [K]_{ii}^{-1}[P]_i \\ [P]_b - [K]_{bi}[K]_{ii}^{-1}[P]_i \end{bmatrix}$$

(A2)

$[K]'_{ib}$ An external node displacement to internal node displacement conversion matrix.

$[K]'_{bb}$ A condensed stiffness matrix of the panel element containing external d.o.f. only, it is the panel element stiffness matrix

$[u]^i_i$ An internal node displacement generated by internal node loads with external nodes being fixed.

$[P]'_b$ A condensed load matrix corresponding to the condensed stiffness matrix $[K]'_{bb}$ for the panel element in global analysis, the number of rows is equal to the external d.o.f.

References

[1] Li TQ. A panel element for parallel finite element analysis. In: Topping BHV, Iványi P, editors. Proceedings of the third international conference on parallel, distributed, grid and cloud computing for engineering. Civil-Comp Press, Stirlingshire, Scotland; 2013. paper 37 doi:10.4203/ccp.101.37.

[2] Allman DJ. A compatible triangular element including vertex rotation for plane elasticity analysis. Comput Struct 1984;19:1–8.

[3] Allman DJ. A Quadrilateral finite element including vertex rotation for plane elasticity analysis. Int J Numer Methods Eng 1988;26:717–30.

[4] Allman DJ. Evaluation of the constant triangle with drilling rotations. Int J Numer Methods Eng 1988;26:2645–55.

[5] Cook RD. On the Allman triangle and a related quadrilateral element. Comput Struct 1986;2:1065–7.

[6] Cook RD. A plane hybrid element with rotational d.o.f. and adjustable stiffness. Int J Numer Methods Eng 1987;24:1499–508.

[7] Richard H. A refined four-noded membrane element with rotational degrees of freedom. Comput Struct 1986;1:75–84.

[8] Zienkiewicz OC, Taylor RL. The finite element method for solid and structural mechanics. 6th ed. 2005.

[9] Guyan RJ. Reduction of stiffness and mass matrices. AIAA J 1965;3(2):80.

[10] Cook RD, Malkus DS, Plesha ME, Witt RJ. Concepts and applications of finite element analysis. 4th ed. 2001.

[11] Oasys Software. GSA Version 8.7. Arup, 13 Fitzroy Street London W1T 4BQ, 2012.